NSSC

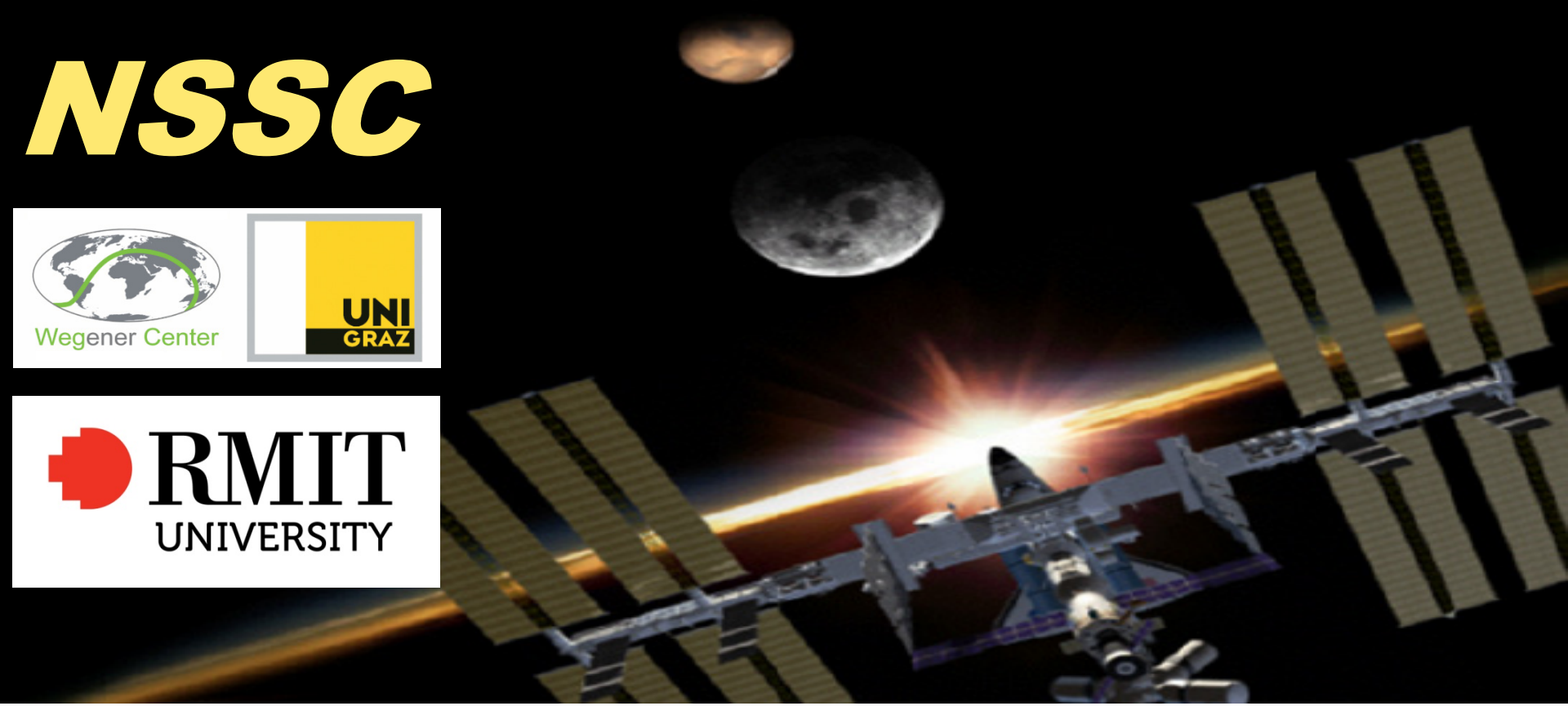

Quantification of Residual Ionospheric Errors in GNSS RO Bending Angles Based on End-to-end Simulation Data

National Space Science Center, CAS

2014.4.16

Quantification of Residual Ionospheric Errors in GNSS RO Bending Angles Based on End-to-end Simulation Data

C. L. Liu[1], G. Kirchengast[2,3,1], K. Zhang[3], W. H. Bai[1], Y. Q. Sun[1], R. Norman[3], Y. Li[4], J. Fritzer[2], M. Schwaerz[2], Z. Q. Wang[5]

1 National Space Science Center (NSSC), Chinese Academy of Sciences, Beijing, China
2 Wegener Center for Climate and Global Change (WEGC) and Institute for Geophysics, Astrophysics, and Meteorology/Inst. of Physics, University of Graz, Graz, Austria
3 SPACE Research Centre, RMIT University, Melbourne, Australia
4 Institute of Geodesy and Geophysics (IGG), Chinese Academy of Sciences, Wuhan, China
5 Beijing Institute of Tracking and Telecommunication Technology

References:
1) Liu, C. L., G. Kirchengast, K. F. Zhang, R. Norman, Y. Li, S. C. Zhang, B. Carter, J. Fritzer, M. Schwaerz, S. L. Choy, S. Q. Wu, and Z. X. Tan (2013), Characterisation of residual ionospheric errors in bending angles using GNSS RO end-to-end simulations, *Adv. Space Res.*, 52, 821-836, doi:10.1016/j.asr.2013.05.021.
2) Liu, C. L., G. Kirchengast, K. Zhang, R. Norman, Y. Li, S. C. Zhang, J. Fritzer, M. Schwaerz, S. Q. Wu, and Z. X. Tan (2015), Quantifying residual ionospheric errors in GNSS radio occultation bending angles based on ensembles of profiles from end-to-end simulations, *Atmos. Meas. Tech. Discuss.*, 8, 759-809, doi:10.5194/amtd-8-759-2015.

Outline

- Residual Ionospheric Errors (RIEs)
- RIEs simulation
- RIEs analysis using single RO events
- RIEs analysis using ensembles of simulated RO data
- Summary and conclusions

Residual Ionospheric Errors

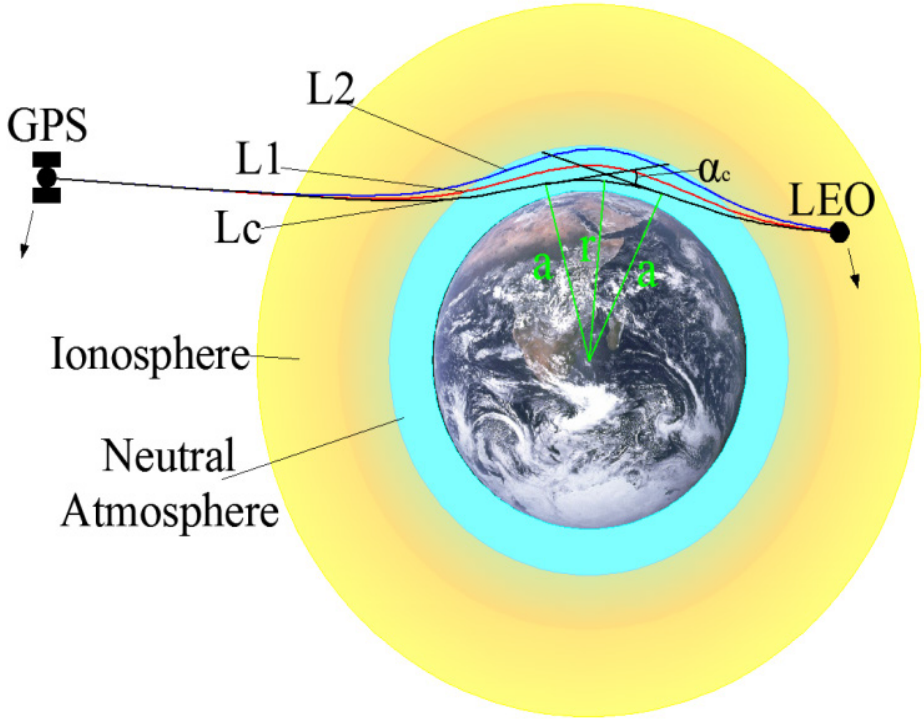

Radio occultation geometry illustrating the separated L1 and L2 signal paths and the ionosphere-corrected ray path Lc

$$\alpha_c(a) = (f_1^2\alpha_1(a) - f_2^2\alpha_2(a))/(f_1^2 - f_2^2)$$

Residual ionospheric errors (RIEs) in GNSS RO retrievals contain:

- The residual first-order effect of a dual-frequency linear combination
- High-order effects which are caused by the uneven distribution and anisotropy of the ionopsheric plasma, respectively.

RIEs simulation

- Simulating no-ionosphere bending angle profiles using MSIS-90 only, for obtaining a reference;
- Simulating ionosphere-corrected bending angle profiles using both MSIS-90 and 3D NeUoG models, and performing the dual-frequency linear combination
- Obtaining the bending angle RIE profiles by differencing the ionosphere-corrected and the no-ionosphere bending angle profiles obtained from the above two steps.

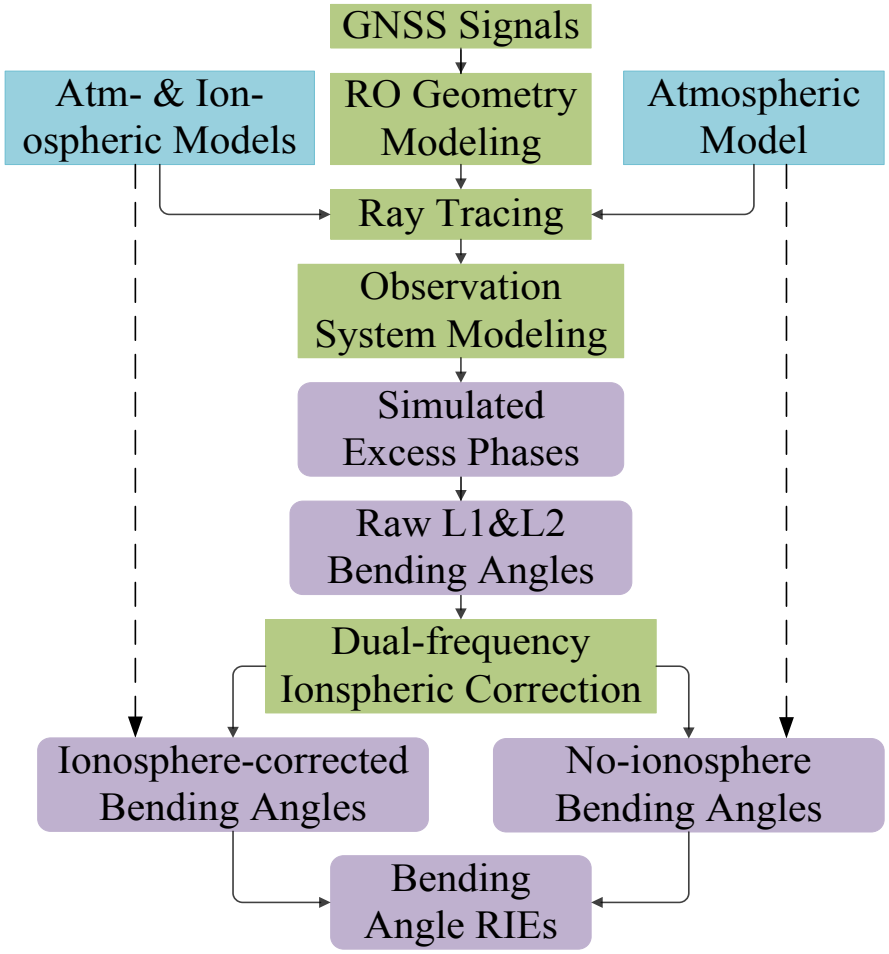

Flow chart of the RO end-to-end simulation process for bending angle RIEs

RIEs analysis using single RO events

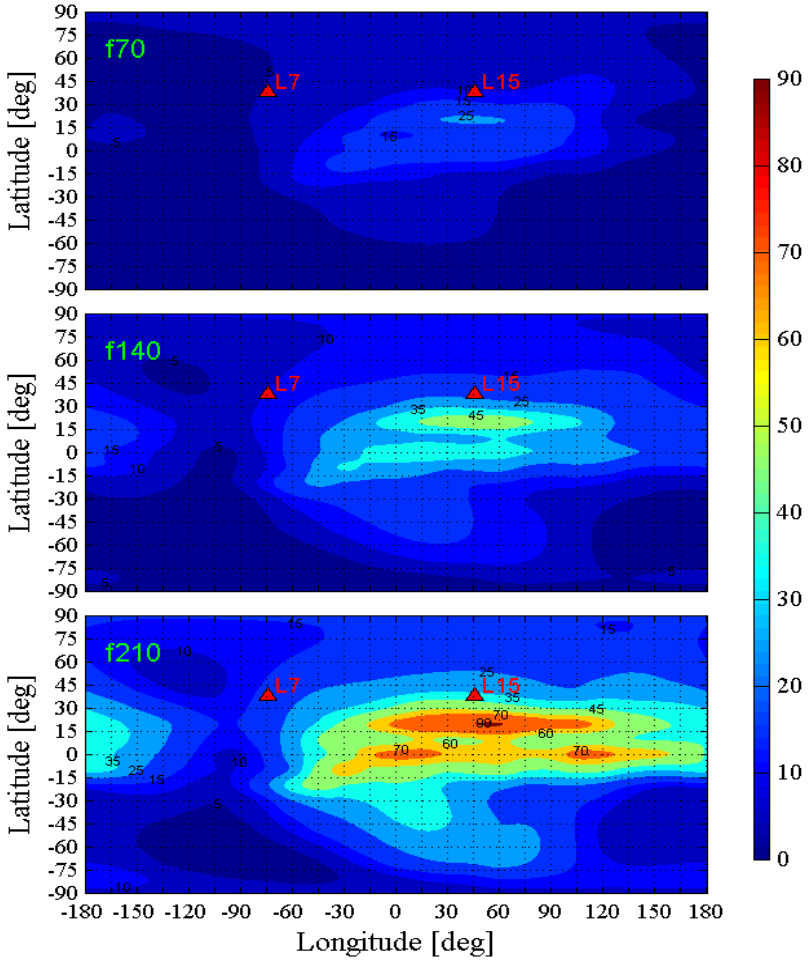

Distributions of 3D NeUoG VTEC for three ionization levels and two RO locations of simulated events

RIEs analysis using single RO events

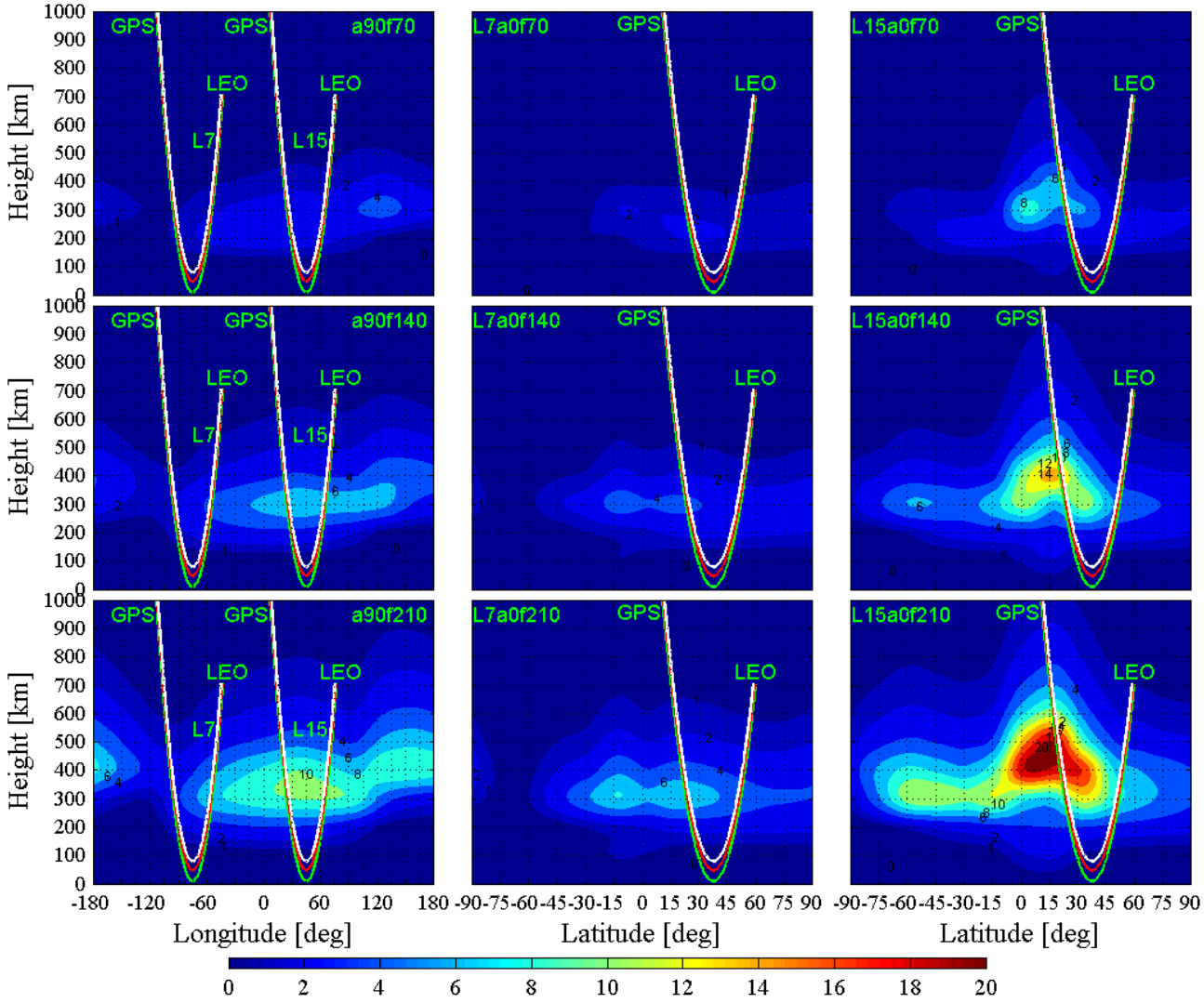

Cross-sectional views of vertical electron density along the ray paths

RIEs analysis using single RO events

Bending angle simulation results for the three morning latitudinal events and comparisons with their reference bending angles in the mesosphere (MS) and upper stratosphere (US) regions.
Each panel row shows the bending angles at all the three ionization levels

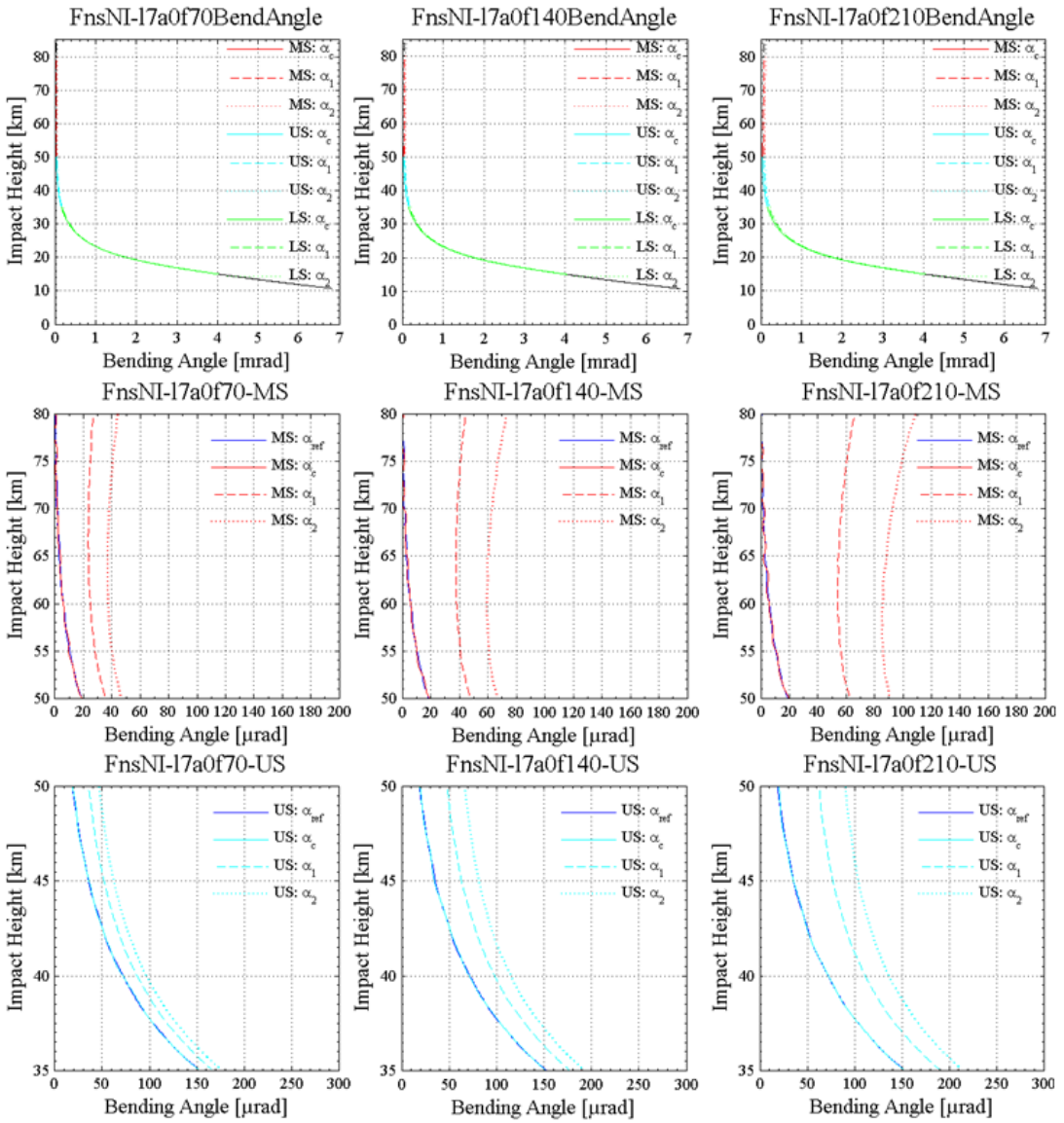

RIEs analysis using single RO events

Bending angle simulation results for the three afternoon longitudinal events and comparisons with their reference bending angles

Absolute and relative bending angle RIE profiles calculated by:

$$\epsilon_a(h_i) = \alpha_c(h_i) - \alpha_{ref}(h_i)$$

$$\epsilon_r(h_i) = 100 * \epsilon_a(h_i) / \alpha_{ref}(h_i)$$

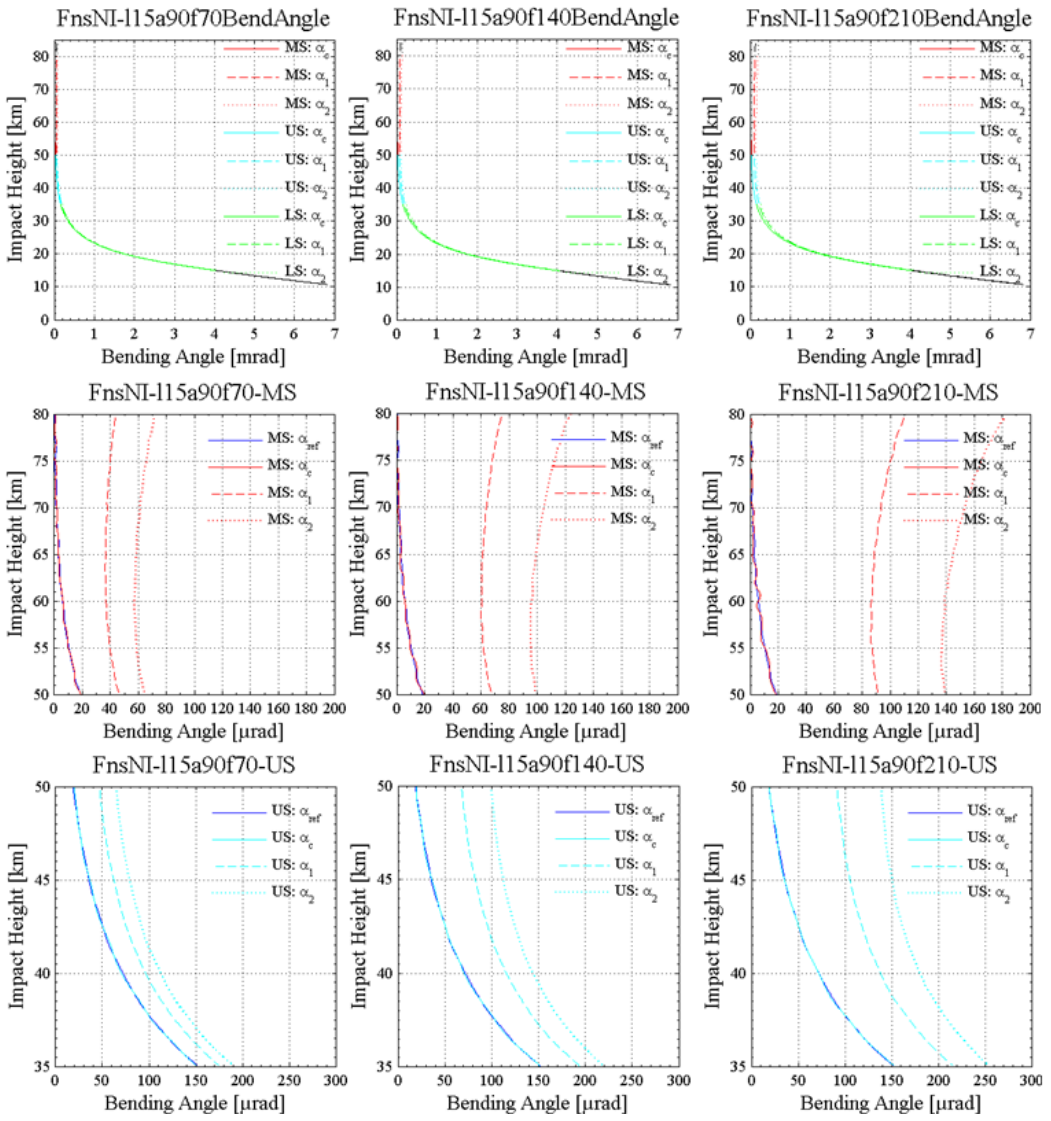

RIEs analysis using single RO events

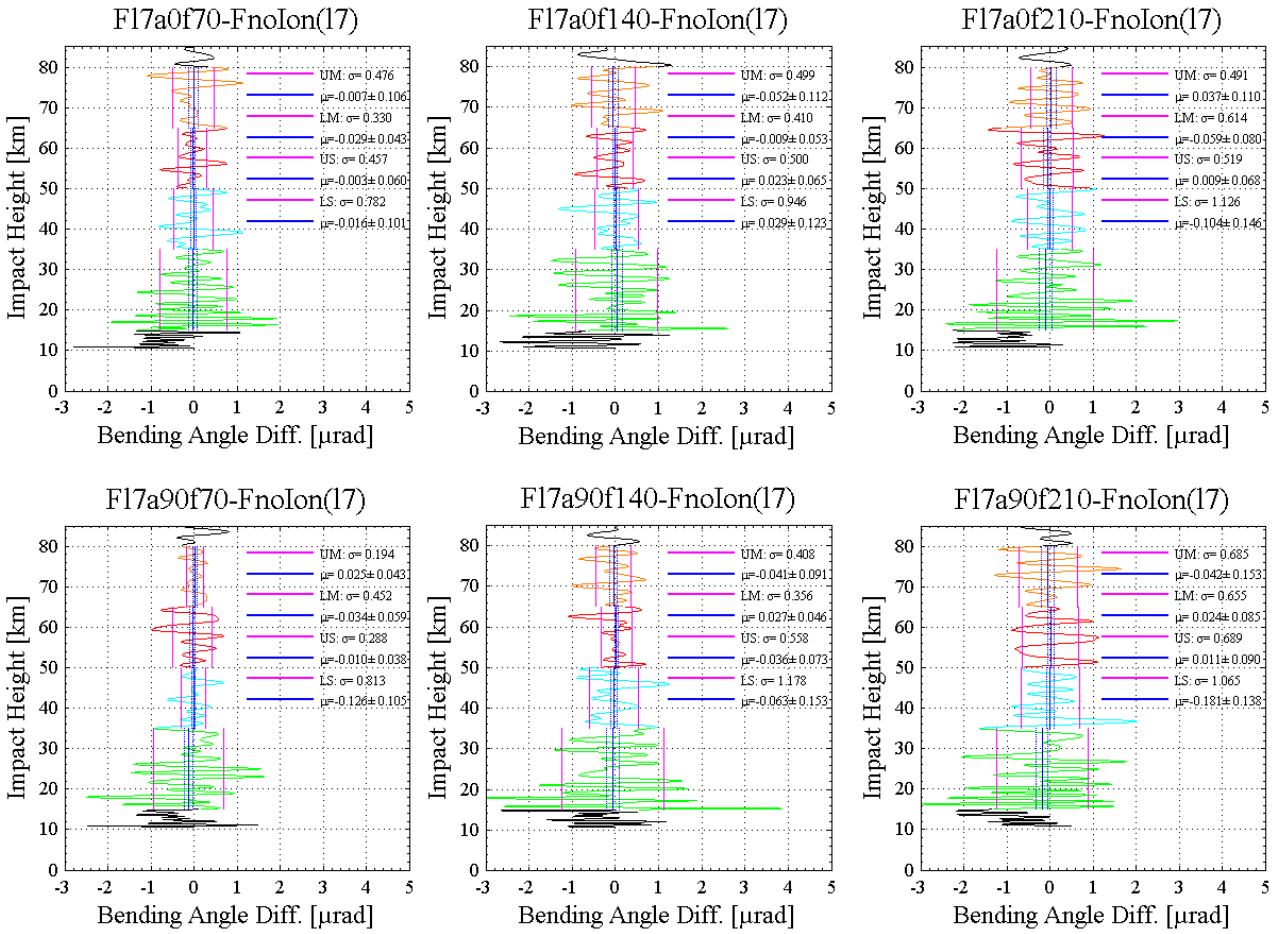

Absolute RIE profiles of the simulated bending angles and their statistical results over four characteristic height layers, lower stratosphere 15–35 km (LS), upper stratosphere 35–50 km (US), lower mesosphere 50–65 km (LM), and upper mesosphere 65–80 km (UM). (Morning/7:00LT RO events)

RIEs analysis using single RO events

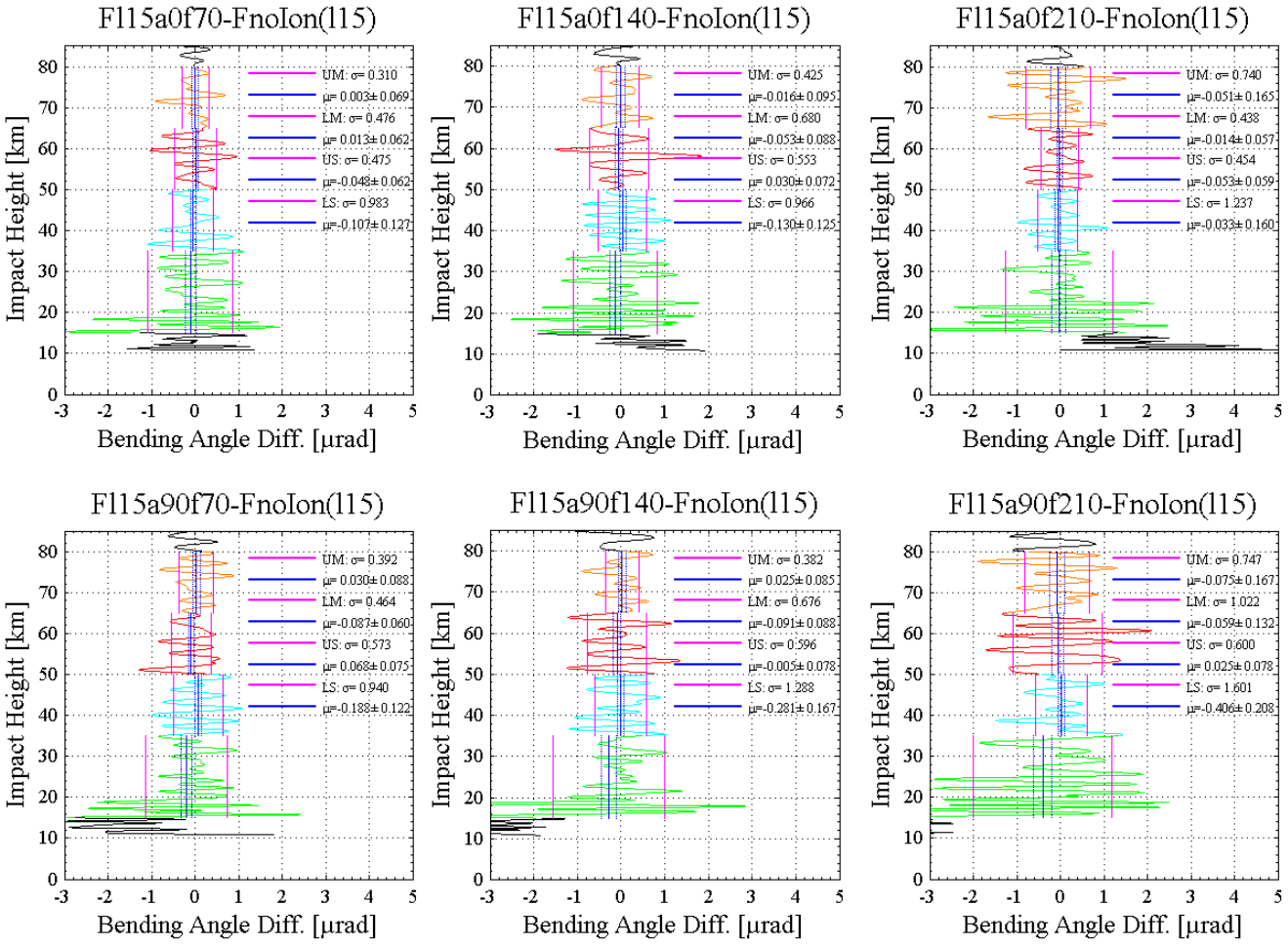

Absolute RIE profiles of the simulated bending angles and their statistical results over four characteristic height layers. (Afternoon/15:00LT RO events)

RIEs analysis using single RO events

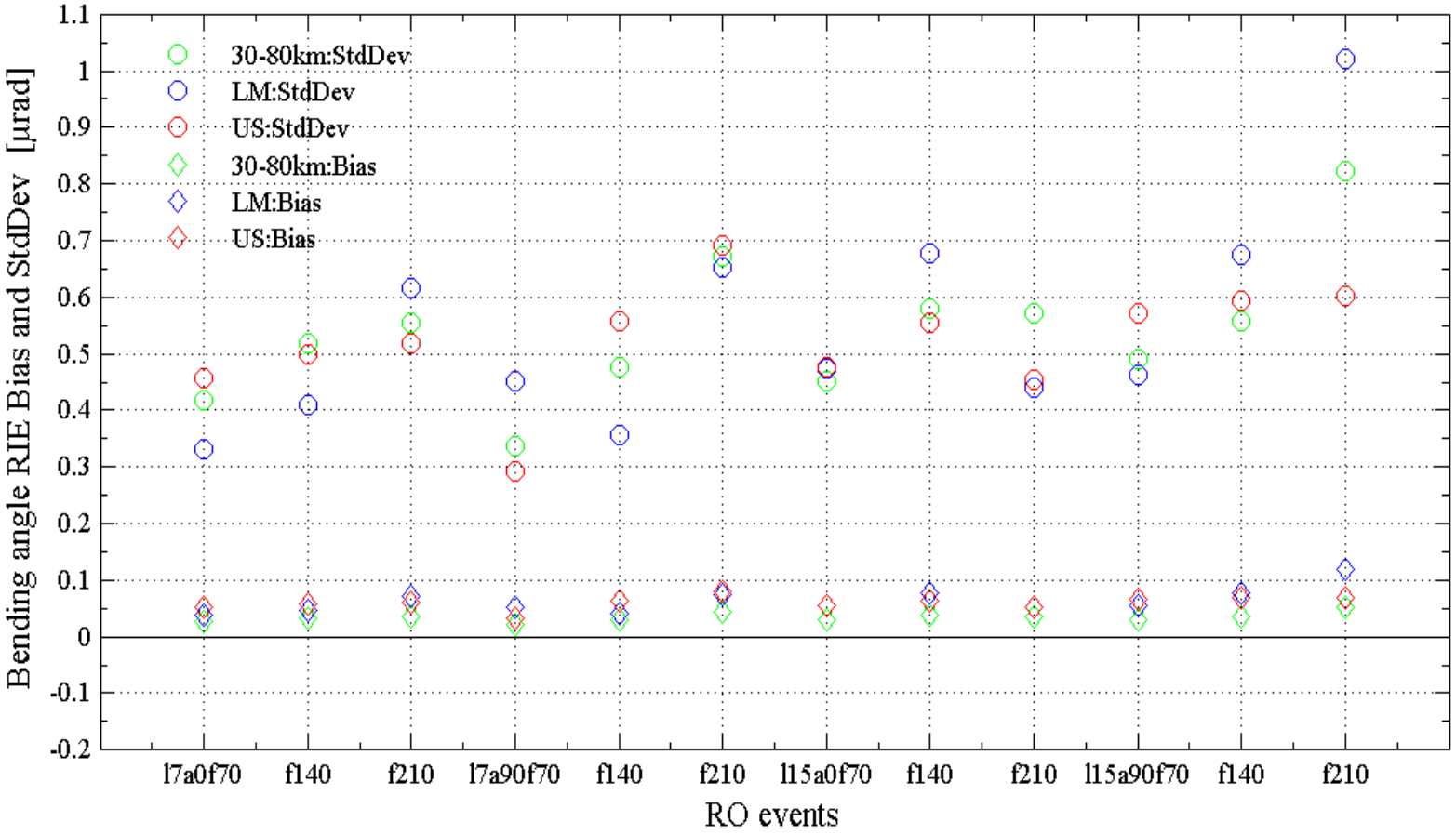

Values of biases (diamond symbols) and standard deviations (circle symbols) of the RIEs for the 12 RO events in the US (red), LM (blue), and 30−80 km impact height range (green), respectively.

RIEs analysis using single RO events

Summary of this section:

- Local time, solar intensity and RO direction are main factors affecting the RIEs
- The afternoon events' RIEs are greater than those of the morning events
- The RIEs at higher solar activity are greater than those from lower activity
- For ray paths under more asymmetric conditions the RIEs tend to be higher

RIEs analysis using ensembles RO data

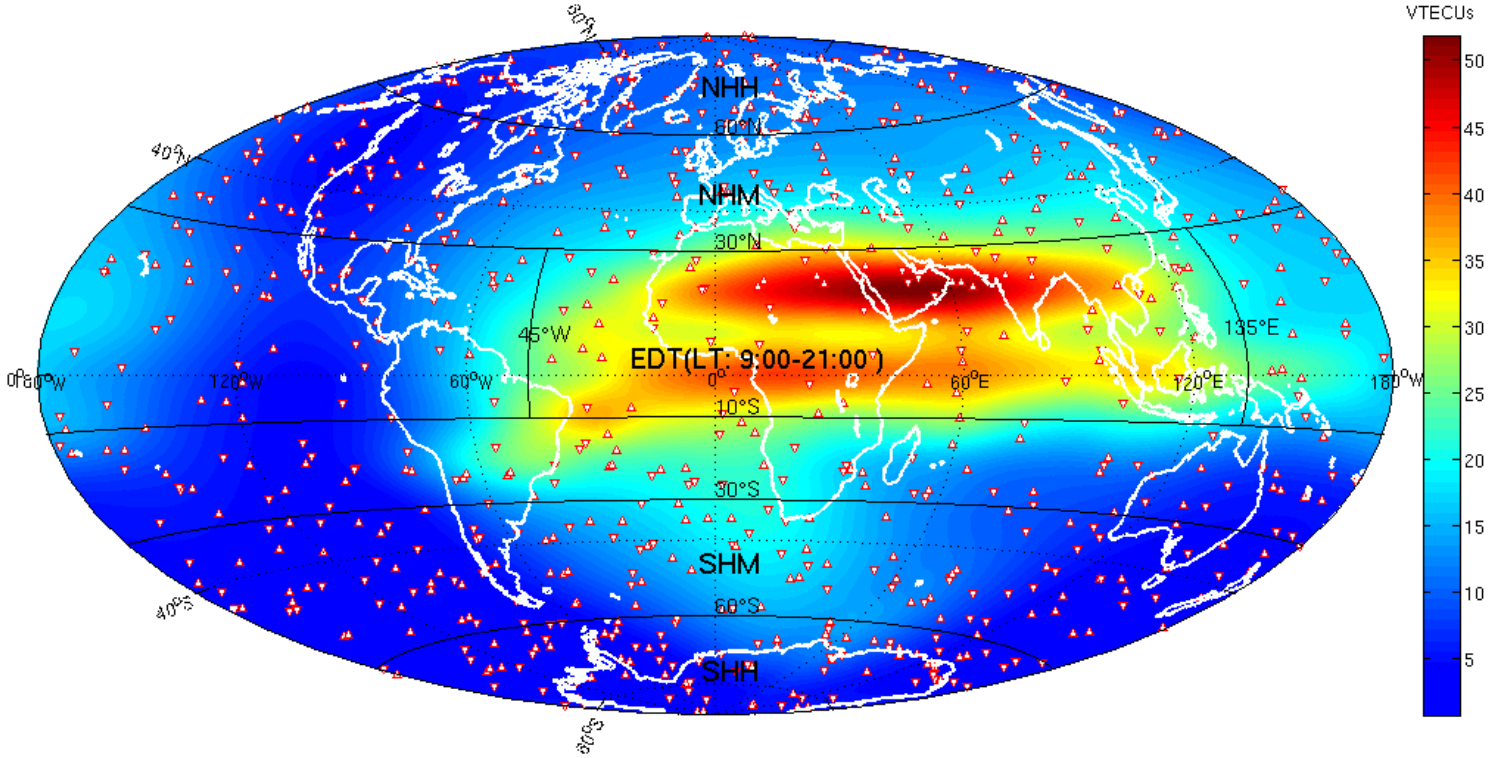

Distribution of the 697 RO events used in the statistical analysis: the upward-pointing triangles denote rising events, the downward-pointing triangles setting events; the 5 latitudinal zones (NHH, NHM, SHM, SHH, EDT) are devided by latitude-circle lines (solid lines), the background colour map illustrates the ionospheric VTEC.

RIEs analysis using ensembles RO data

Geographic zone definitions

Abbreviation	Zone	Latitude range	Longitude (LT) range
GLO	Global	90° S – 90° N	180° W – 180° E
NHH	Northern Hemisphere High-latitude	60° N – 90° N	180° W – 180° E
NHM	Northern Hemisphere Middle-latitude	30° N – 60° N	180° W – 180° E
EDT	Equatorial Day Time	10° S – 30° N	9:00 – 21:00 LT
SHM	Southern Hemisphere Middle-latitude	30° S – 60° S	180° W – 180° E
SHH	Southern Hemisphere High-latitude	60° S – 90° S	180° W – 180° E

RIEs analysis using ensembles RO data

Definition of end-to-end simulation cases for various ionospheric conditions and solar activity levels under the assumptions of no observing system errors or realistic observing system errors.

Abbreviation	Case	Atmo. / Iono. / Obs.Err. model	Solar activity levels
opwi	obs.system perfect, without ionosphere	MSIS-s / no iono. / no obs.err.	–
opss	obs.system perfect, spherical symmetry iono.	MSIS-s / NeUoG-s / no obs.err.	f70, f140, f210
opns	obs.system perfect, nonspherical symmetry iono.	MSIS-s / NeUoG / no obs.err.	f70, f140, f210
orwi	obs.system realistic, without ionosphere	MSIS-s / no iono. / GRAS err.	–
orss	obs.system realistic, spherical symmetry iono.	MSIS-s / NeUoG-s / GRAS err.	f70, f140, f210
orns	obs.system realistic, nonspherical symmetry iono.	MSIS-s / NeUoG / GRAS err.	f70, f140, f210

Level-average bending angle RIE bias, standard deviation (stdσ) and 2σ confidence-level uncertainty are calculated by:

$$\left.\begin{aligned}\bar{\epsilon}_a(h_i) &= \sum_{j=1}^{n}\epsilon_{aj}(h_i)/n \\ \bar{\epsilon}_r(h_i) &= \sum_{j=1}^{n}\epsilon_{rj}(h_i)/n\end{aligned}\right\} \qquad \sigma(h_i) = \sqrt{\sum_{j=1}^{n}\left(\epsilon_j(h_i)-\bar{\epsilon}_j(h_i)\right)^2/(n-1)} \qquad 2\sigma un(h_i) = 2\sigma(h_i)/\sqrt{n}$$

RIEs analysis using ensembles RO data

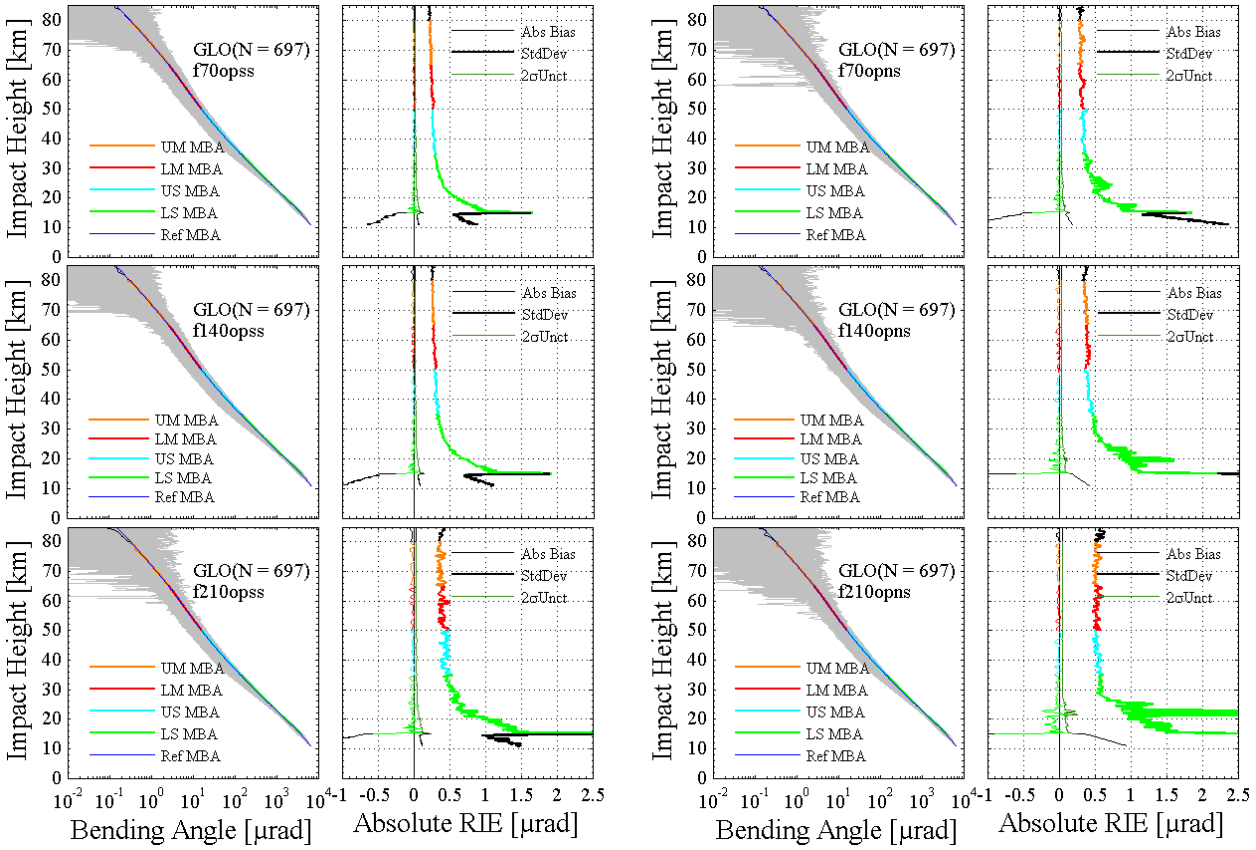

Ionosphere-corrected bending angle profiles and their statistical results for the global ensemble 'opss' dataset (left) and 'opns' dataset (right).

RIEs analysis using ensembles RO data

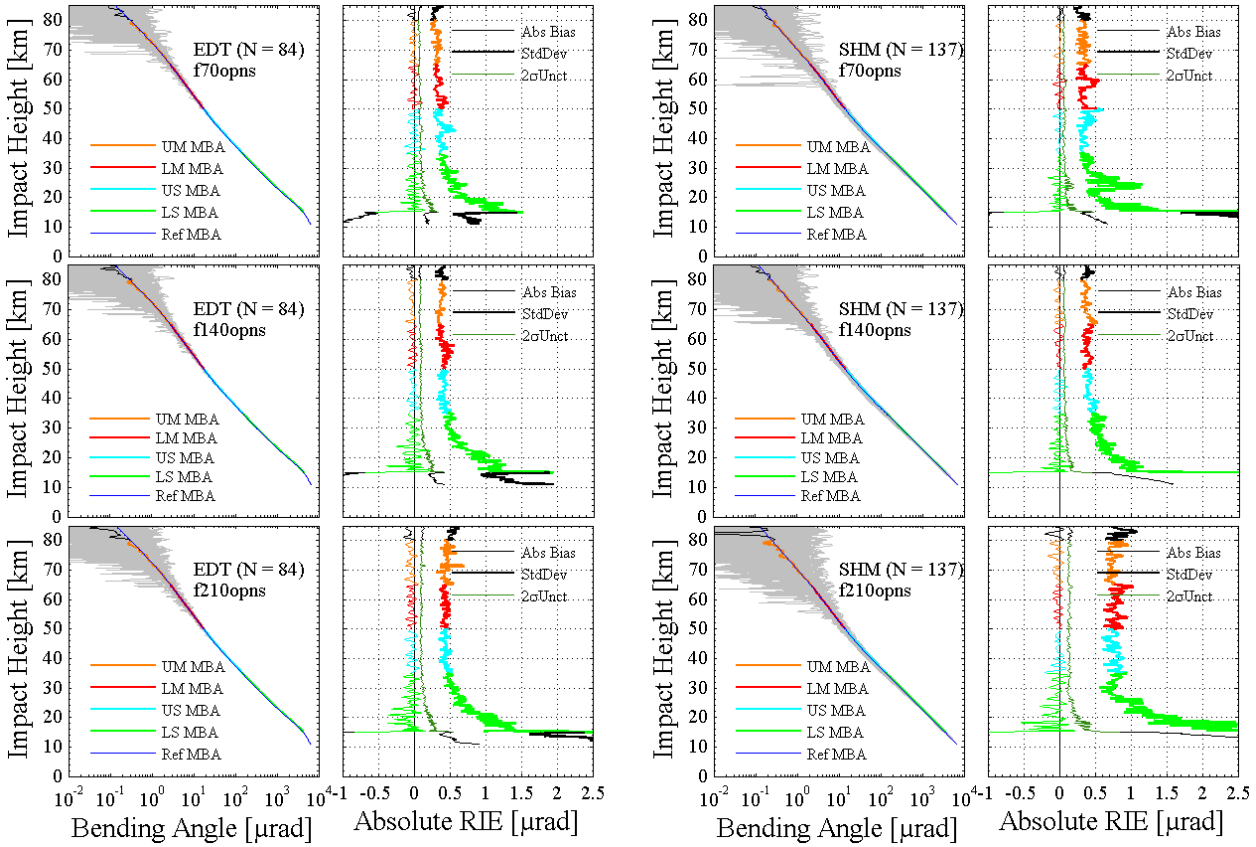

Ionosphere-corrected bending angle profiles and their statistical results for the EDT (left) and SHM (right) 'opns' datasets.

RIEs analysis using ensembles RO data

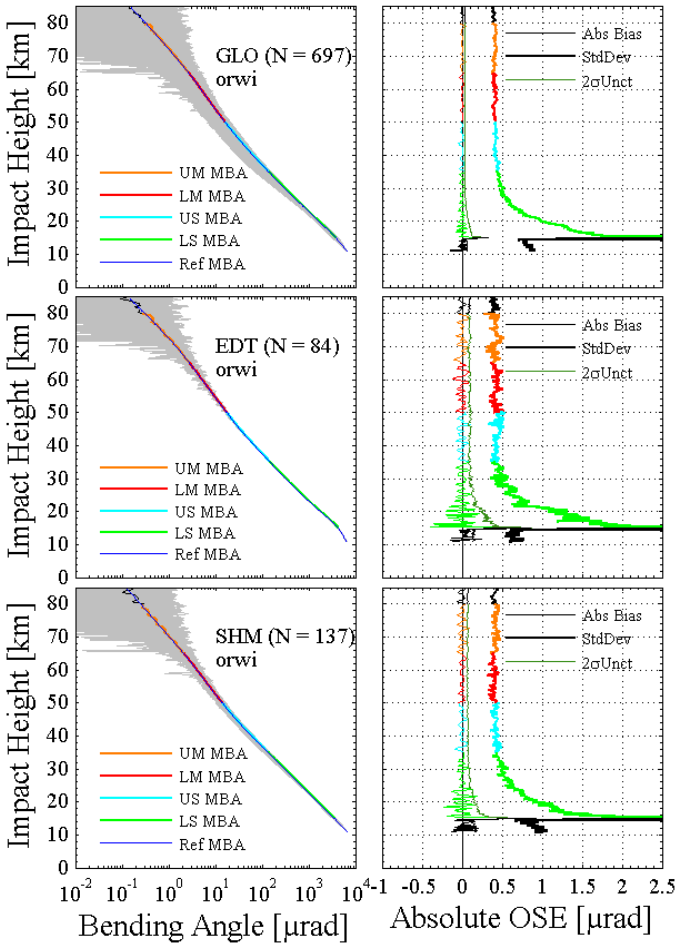

Ionosphere-corrected bending angle profiles and their statistical results for the 'orwi' dataset.

RIEs analysis using ensembles RO data

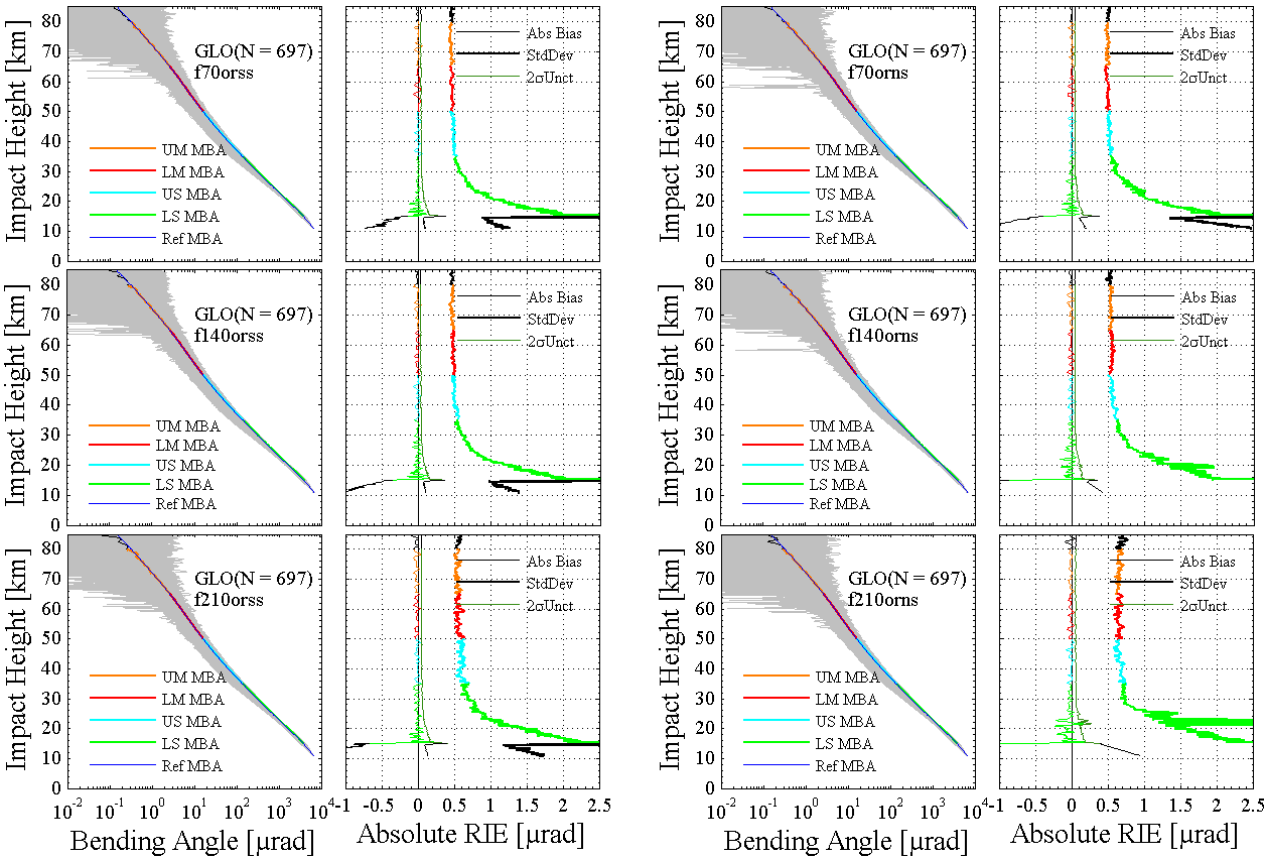

Ionosphere-corrected bending angle profiles and their statistical results for the GLO ‘orss’ (left) and ‘orns’ (right) datasets.

RIEs analysis using ensembles RO data

Bending angle residual ionospheric error (RIE) estimates for realistic observing system and nonspherical symmetry case (orns)

Height layer [km]	Low solar activity (F10.7=70) Abs. RIE [μrad] bias±2σstdev	Low solar activity (F10.7=70) Rel. RIE [%] bias±2σstdev	Medium solar activity (F10.7=140) Abs. RIE [μrad] bias±2σstdev	Medium solar activity (F10.7=140) Rel. RIE [%] bias±2σstdev	High solar activity (F10.7=210) Abs. RIE [μrad] bias±2σstdev	High solar activity (F10.7=210) Rel. RIE [%] bias±2σstdev
GLO (90 ° S – 90 ° N; *N*=697, *n*=10455)						
65 to 80	–0.003±0.009 0.48	–0.22±1.34 68.7	–0.013±0.010 0.53	–1.96±1.44 73.8	–0.019±0.013 0.64	–2.50±1.82 93.2
50 to 65	–0.004±0.010 0.49	–0.08±0.18 9.45	–0.012±0.011 0.55	–0.22±0.21 10.5	–0.021±0.013 0.64	–0.37±0.24 12.5
35 to 50	–0.003±0.010 0.51	–0.01±0.03 1.45	–0.008±0.011 0.56	–0.02±0.03 1.53	–0.015±0.013 0.66	–0.03±0.04 1.80
20 to 35	–0.007±0.014 0.74	0.00±0.01 0.18	–0.012±0.016 0.84	0.00±0.01 0.19	–0.038±0.022 1.10	–0.01±0.01 0.23
NHH (60 ° N – 90 ° N; *N*=86, *n*=1290)						
65 to 80	–0.004±0.027 0.49	–0.43±2.24 40.3	–0.006±0.028 0.51	–1.03±2.28 40.9	–0.019±0.031 0.55	–2.02±2.48 44.6
50 to 65	–0.004±0.026 0.47	–0.11±0.34 6.04	–0.016±0.028 0.51	–0.28±0.37 6.69	–0.024±0.032 0.57	–0.31±0.41 7.36
35 to 50	–0.005±0.030 0.53	–0.01±0.06 1.11	–0.001±0.031 0.56	–0.01±0.07 1.19	–0.007±0.033 0.60	0.00±0.07 1.25
20 to 35	–0.008±0.040 0.72	0.00±0.01 0.16	–0.010±0.046 0.83	0.00±0.01 0.19	–0.014±0.050 0.89	0.00±0.01 0.20
NHM (30 ° N – 60 ° N; *N*=135, *n*=2025)						
65 to 80	–0.007±0.021 0.48	–0.49±2.20 49.5	–0.021±0.024 0.53	–2.17±2.44 54.8	–0.039±0.023 0.52	–4.63±2.40 54.1
50 to 65	–0.005±0.021 0.48	–0.12±0.31 6.94	–0.015±0.025 0.56	–0.16±0.36 8.14	–0.030±0.023 0.52	–0.47±0.34 7.61
35 to 50	–0.012±0.023 0.51	–0.03±0.05 1.15	–0.006±0.025 0.56	–0.01±0.06 1.24	–0.022±0.025 0.57	–0.04±0.06 1.27
20 to 35	–0.015±0.034 0.76	0.00±0.01 0.17	–0.014±0.039 0.87	0.00±0.01 0.18	–0.028±0.036 0.80	–0.01±0.01 0.18
EDT (10 ° S – 30 ° N; 9:00 LT – 21:00 LT; *N*=84, *n*=1260)						
65 to 80	–0.017±0.028 0.50	–2.60±3.36 59.6	–0.036±0.031 0.55	–4.84±4.05 71.8	–0.052±0.034 0.61	–6.89±4.36 77.3
50 to 65	–0.010±0.028 0.50	–0.23±0.47 8.36	–0.024±0.032 0.56	–0.36±0.51 9.09	–0.043±0.033 0.58	–0.75±0.53 9.44
35 to 50	–0.001±0.030 0.54	0.00±0.07 1.30	–0.019±0.031 0.55	–0.04±0.07 1.33	–0.036±0.034 0.60	–0.09±0.08 1.45
20 to 35	–0.016±0.043 0.77	0.00±0.01 0.17	–0.017±0.046 0.82	0.00±0.01 0.19	–0.061±0.051 0.90	–0.01±0.01 0.20
SHM (30 ° S – 60 ° S; *N*=137, *n*=2055)						
65 to 80	–0.002±0.022 0.50	–0.14±3.75 85.0	–0.021±0.023 0.53	–4.40±3.86 87.5	–0.036±0.037 0.83	–6.60±6.01 136.3
50 to 65	–0.007±0.023 0.51	–0.19±0.48 10.9	–0.007±0.024 0.54	–0.16±0.51 11.5	–0.021±0.038 0.86	–0.46±0.80 18.2
35 to 50	–0.005±0.023 0.52	–0.01±0.07 1.59	–0.016±0.026 0.58	–0.05±0.07 1.64	–0.020±0.037 0.84	–0.06±0.11 2.40
20 to 35	–0.001±0.034 0.77	0.00±0.01 0.19	–0.017±0.035 0.80	0.00±0.01 0.20	–0.044±0.046 1.05	–0.01±0.01 0.26
SHH (60 ° S – 90 ° S; *N*=99, *n*=1485)						
65 to 80	0.003±0.023 0.44	1.28±5.09 98.1	–0.001±0.023 0.44	–0.09±5.01 96.6	0.002±0.025 0.49	0.47±5.63 108.5
50 to 65	–0.001±0.023 0.45	–0.04±0.74 14.2	–0.006±0.024 0.46	–0.25±0.79 15.2	–0.003±0.024 0.47	–0.21±0.77 14.8
35 to 50	0.002±0.024 0.46	0.00±0.11 2.09	–0.004±0.024 0.46	–0.02±0.11 2.10	0.001±0.025 0.48	0.00±0.11 2.21
20 to 35	–0.007±0.033 0.64	0.00±0.01 0.21	0.002±0.042 0.80	0.00±0.01 0.22	–0.005±0.076 1.46	0.00±0.02 0.30

RIEs analysis using ensembles RO data

Relationship between the histogram distribution of the number of RO events and the bias (left panels) and STD (right panels) of the bending angle RIEs, in the UM from the GLO f70opns, GLO f210opns, GLO opwi, GLO f70orns, and GLO f210orns datasets (top to bottom).

The red, blue and green lines denote layer-average, event-average and median biases (left panels) and standard deviations (right panels) of bending angle RIEs, respectively.

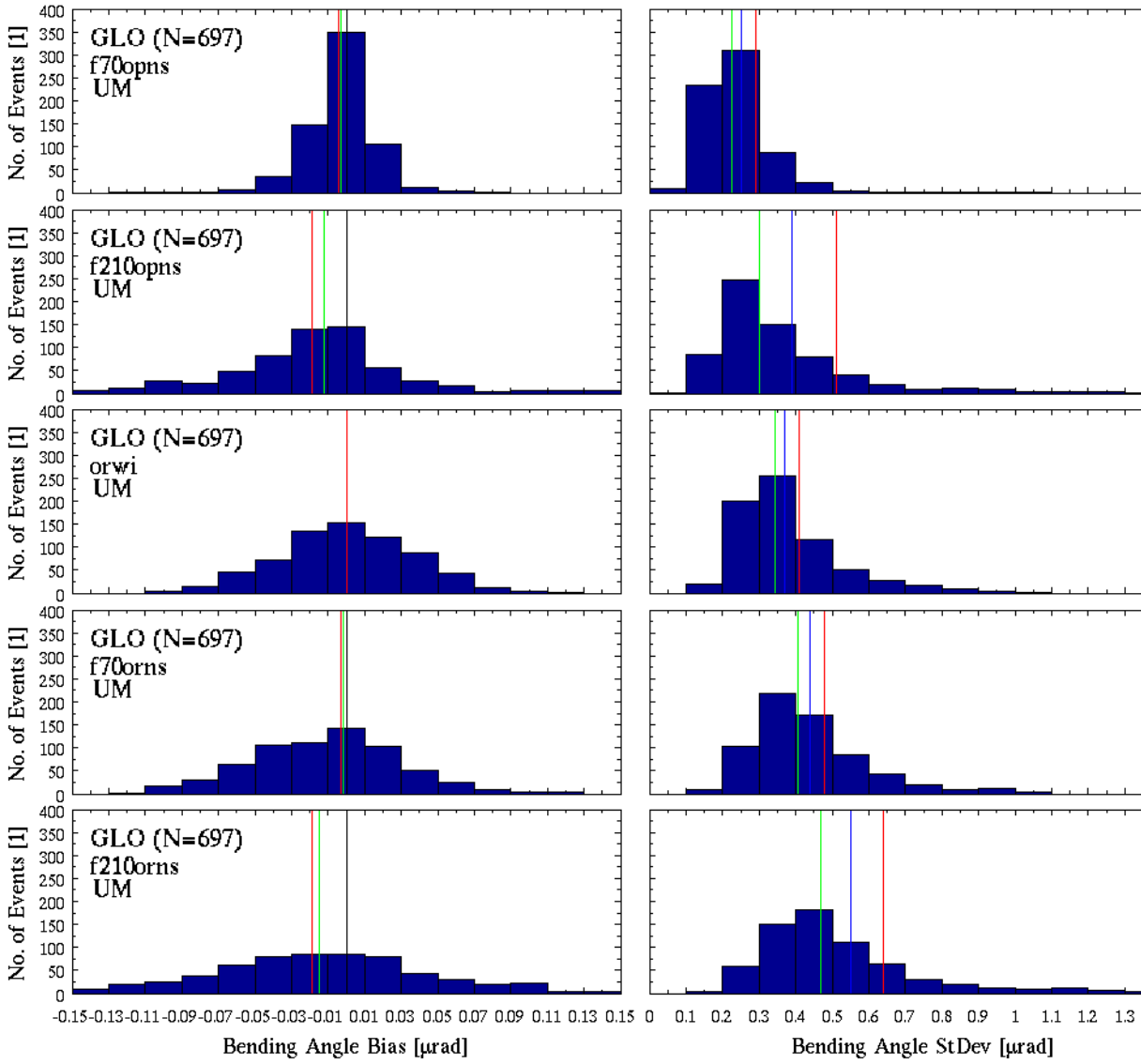

Summary and conclusions

- The mean bending angle RIE biases have a negative tendency, leading to systematic errors.
- The bending angle RIE biases and their STDs increase with increasing solar activity.
- The EDT data zone shows the largest RIE biases.
- The RIE biases in middle latitude data zones are slight smaller than those in the EDT, while their STDs are slightly larger.
- The results help to inform future RIE mitigation schemes that will improve upon the use of the linear ionospheric correction of bending angles.

Thank you!